

# A New Tool for Nonlinear Dynamical Analysis of Heart Rate Variability

A. Posiewnik and J. Dąbkowski

Institute of Theoretical Physics and Astrophysics, University of Gdańsk, 80-952 Gdańsk, Wita Stwosza 57, Poland

Z. Naturforsch. **53a**, 112–116 (1998); received November 29, 1997

In this paper we analyse the sequences of the time intervals between heart-beats-the RR intervals- by means of AIP (artificial insymmetration patterns) diagrams.

The sequences were produced by artificial heartbeat sequences generated numerically and compared with sequences obtained from real heart activity.

We hope that the AIP diagrams method will prove useful for a rapid qualitative assessment of dynamics from nonlinear time series, and that it is able to distinguish various types of heart dynamics (regular and pathological), while other diagnostical methods fail.

In industrial countries, sudden cardiac death (SCD) is a frequent cause of death among men aged 20–60 years. So it is important to recognize patients with high risk of SCD as early and reliably as possible.

The analysis of electrocardiogram (ECG) data may be divided into two basic areas. In morphological analysis the shape of electrical pulses measured is examined [1]. The method is based on the computation of the respective Shannon entropies and often provides a sharp distinction between healthy persons and patients with high risk of SCD. On the other hand, in the complementary type of ECG analysis the time distances between heartbeats – the RR intervals – are measured [2].

Three-dimensional images in the phase space are formed by means of the Takens-Ruelle reconstruction method of long sequences of cardiac interbeat intervals [3]. Projections of the three-dimensional images of the RR sequences could serve as a diagnostic tool of different cases of cardiac arrhythms [3, 4].

In this paper we used the algorithm for so called artificial insymmetration patterns in order to analyse RR sequences.

Artificial *insymmetration* patterns (AIP) (also known as symmetrized dot patterns), have been introduced by Pickover [5] as a qualitative method of visualizing correlation functions in time series data. For the interpretation of underlying patterns, the data are mapped in a manner which artificially induces symmetry into the data set.

This artificial symmetry is statistically enhanced for portions of the time series signal that have a high probability of contributing to the underlying signal, while

those data points dominated by noise produce a scattered field with no underlying symmetry. The algorithm is implemented by working with only a single channel of data. We process the data by selecting sequential points in the data set to be the radius and angle coordinates in polar space.

The first value is the radius while the second is used as the angle. The angle point is also duplicated by a second point with an opposing sign value. The resulting polar spatial distribution is reproduced around the polar center for an arbitrary number of times, by specifying the number of segments the 360 degree circle is to be divided into. 60 degrees seems to be a good working number, although in practice 120 degrees was found to enhance certain data structures.

The AIP transformation is given by

$$\mathbf{x}: F(t) \rightarrow S(r_j, \Theta_{ij}, \Phi_{ij})$$

where  $F(t)$  represents the discrete time series, and  $S$  is the AIP.  $S$  is a traditional function of  $r$  in radial vector polar coordinates, while  $\Theta$  and  $\Phi$  are two polar angles obtained by Pickovers's transformation:

$$r_j = \frac{F_j - L}{H - L} \xi,$$

$$\Theta_{ij} = \Theta^i \frac{F_{j+1} - L}{H - L} \xi,$$

$$\Phi_{ij} = \Theta^i \frac{F_{j+1} - L}{H - L} \xi,$$

where  $j = 1, 2, 3, \dots, N - 1$ .

$$\Theta^i = (360^\circ/m) i, \quad i = 1, 2, 3, \dots, m.$$

Reprint requests to A. Posiewnik; e-mail: fizap@paula.univ.gda.pl; Fax: 485 83 41 31 75.

0932-0784 / 98 / 0300-0112 \$ 06.00 © – Verlag der Zeitschrift für Naturforschung, D-72027 Tübingen



Dieses Werk wurde im Jahr 2013 vom Verlag Zeitschrift für Naturforschung in Zusammenarbeit mit der Max-Planck-Gesellschaft zur Förderung der Wissenschaften e.V. digitalisiert und unter folgender Lizenz veröffentlicht: Creative Commons Namensnennung-Keine Bearbeitung 3.0 Deutschland Lizenz.

Zum 01.01.2015 ist eine Anpassung der Lizenzbedingungen (Entfall der Creative Commons Lizenzbedingung „Keine Bearbeitung“) beabsichtigt, um eine Nachnutzung auch im Rahmen zukünftiger wissenschaftlicher Nutzungsformen zu ermöglichen.

This work has been digitalized and published in 2013 by Verlag Zeitschrift für Naturforschung in cooperation with the Max Planck Society for the Advancement of Science under a Creative Commons Attribution-NoDerivs 3.0 Germany License.

On 01.01.2015 it is planned to change the License Conditions (the removal of the Creative Commons License condition “no derivative works”). This is to allow reuse in the area of future scientific usage.

Here  $N$  is the number of points in the time series,  $m$  is the number of symmetric mirrored or conjugate plane reflections,  $H$  the maximum value in the data set,  $L$  the minimum value in the data set, and  $\xi$  represents the maximum value used to normalize or scale the data. Pickover suggests that  $\xi \geq 360/m$ , which was found to be a good working figure of merit.

The resulting AIP image can be used to visually discriminate data sets that appear very similar and virtually indistinguishable in a time series. The actual symmetric dot patterns by themselves are of limited use since they do not quantify the underlying data but rather only provide a qualitative insight. Jaenisch has suggested that such patterns may lend themselves to processing and recognition by neural networks [6].

He also proposed to characterize AIP patterns in terms of correlation functions and fractal dimensions using optical parallel processing. Such techniques would enable real time processing using collected data mapped into an AIP.

We investigated the characterization of AIP patterns by means of histograms – and results were very encouraging.

We used a simple algorithm for which the Fortran 77 code is provided by Pickover\*. In practice, good AIP patterns require approximately 200 points to produce reliable characteristics; however, smaller data sets were also used, instead of sufficient initial data, and the results were encouraging.

We checked our method by applying it to numerically created data and comparing them with digitized electrocardiograms obtained from patients with different pathological heart rhythms.

AIP diagrams can assess subtle correlations which may exist in data sets and are not easily detectable with other techniques. The AIP algorithm is very simple and computationally inexpensive, and it can also be applied to short data sets which could be purely deterministic, stochastic or mixed, and not necessarily stationary. The method has a very appealing “visual” aspect. It is our hope that the AIP diagrams could distinguish between various cases of pathology and health, often also in cases where other methods fail.

AIP diagrams obtained from artificially generated heart beat sequences can be used as a catalogue since by its construction the nature of each pattern is well defined.

\* The Fortran 77 code for AIP algorithm is available upon request; contact A. Posiewnik (e-mail: fizap@paula.univ.gda.pl.)

AIP diagrams obtained from real ECG series could thus be compared with this catalogue and a possible corresponding disease be identified.

In our analysis we used artificial heart beat sequences generated according to the prescriptions given in the Grossmann-Ranft paper [7]. There are four main classes of sequences, and we now give a short description of each.

### 1. Sinus Rhythm

All RR intervals  $x_n$ ,  $n = 1, 2, \dots$  are equal but are polluted by noise of physiological origin. So RR intervals are presented by the map

$$x_{n+1} = x_n - c \cdot (x_n - 1) + \sigma \cdot \zeta_n,$$

$$x_n \in [0, 2], n = 0, 1, 2, \dots, c \ll \sigma.$$

Here  $\zeta_n$  is normalized gaussian white noise  $\langle \zeta_n \rangle = 0$ ,  $\langle \zeta_n, \zeta_m \rangle = \delta_{nm}$  and  $\sigma$  is its strength. The restoring term  $c(x_n - 1)$  prevents the signal sequence from diffusional broadening.

This model [7] generates a sort of cudgel in the phase space diagram, Figure 1. We generated the AIP diagrams for the model, choosing different values of  $c$ ,  $\sigma$  and compared them with AIP diagrams obtained from ECG's of healthy persons. It is easy to see the structural similarity of all these diagrams, Fig. 2a, 2b.

### 2. Extrasystoles with Fixed Coupling

Extrasystoles are extra beats of the heart. Unlike for the sinus rhythm, their electrical origin is not the sinus node. Grossmann and Ranft [7] used the following algorithm for generating heart beat sequences with extrasystoles:

- If the last heart beat was an extrasystole, then a compensatory pause will follow.
- If the last heart beat was *not* an extrasystole, then the next one will again be a sinus beat with probability  $p$  and an extrasystole with probability  $1-p$ .

The generated RR sequence typically reads: “. . .  $x$   $x$   $y$   $2x-y$   $x$   $y$   $2x-y$   $x$  . . .” where  $x$  is the distance between two successive sinus beats,  $y$  is the time lag between an extrasystole and the preceding beat (ectopic beat), denoted as *coupling interval*,  $2x-y$  is the length of the compensatory pause to follow,  $y = y_0$  is constant (fixed coupling interval). The sinus beats are again modelled by the sequence  $x_n$  from class 1.

In the phase space diagrams one now obtains four cudgels in the projection on the  $(x_n, x_{n+1})$  coordinate plane, Figure 3. The corresponding AIP diagrams created by ar-

tificial sequences are presented in Fig. 4a and the AIP diagrams obtained from E-CG's of long-time survivors are presented in Figure 4b. As in class 1, one can easily see the apparent structural similarity.

### 3. Extrasystoles with Variable Coupling

- One can choose a constant sinus rhythm  $x_0$  and admit variable coupling intervals. The successive coupling intervals are then modelled by the same algorithm as for the sinus rhythm in class 1.
- Alternatively, both  $x$  and  $y$  are taken as variable, i.e.  $x$  and  $y$  are generated by the noise polluted model from

class 1. For the frequency of the extrasystole occurrence we used the  $(p, 1-p)$  algorithm.

A typical phase-space diagram is given in Figure 5. The corresponding AIP diagrams for artificially generated sequences and for severely ill patients are displayed in Figs. 6a and 6b.

### 4. Conclusions

1. From our analysis we conclude, similarly to Grossmann and Ranft, that one can represent different pathologies in heart beat sequences by simple models with noise polluted regular beats eventually with occasional extra-

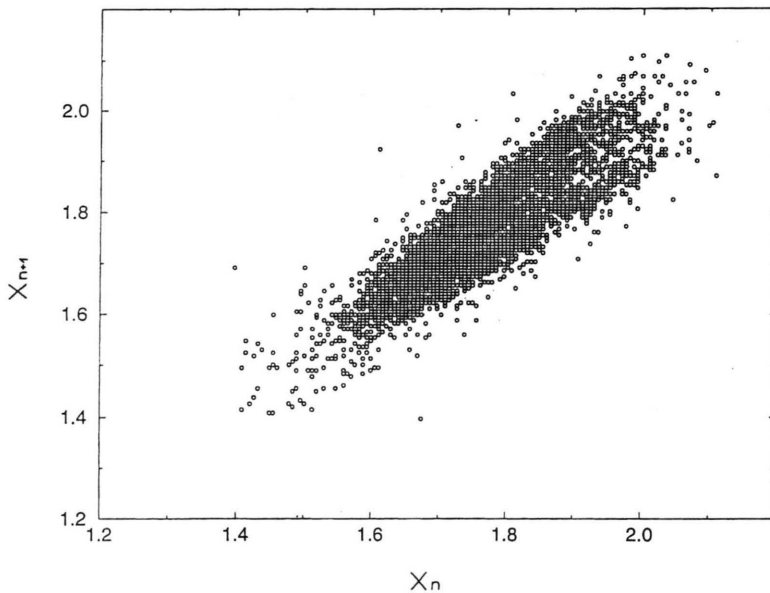


Fig. 1. Phase space diagram of class 1.

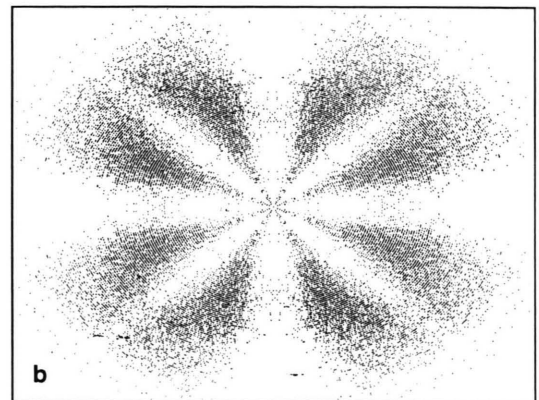
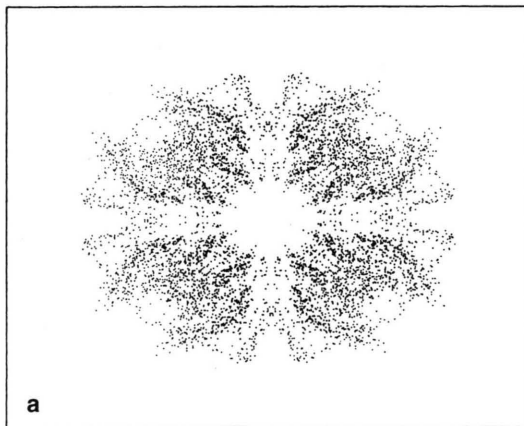


Fig. 2a. AIP diagram of class 1 generated by artificial data using  $c = 0.006$ ,  $\sigma = 0.02$ .

Fig. 2b. AIP diagram of real ECG data from healthy person.

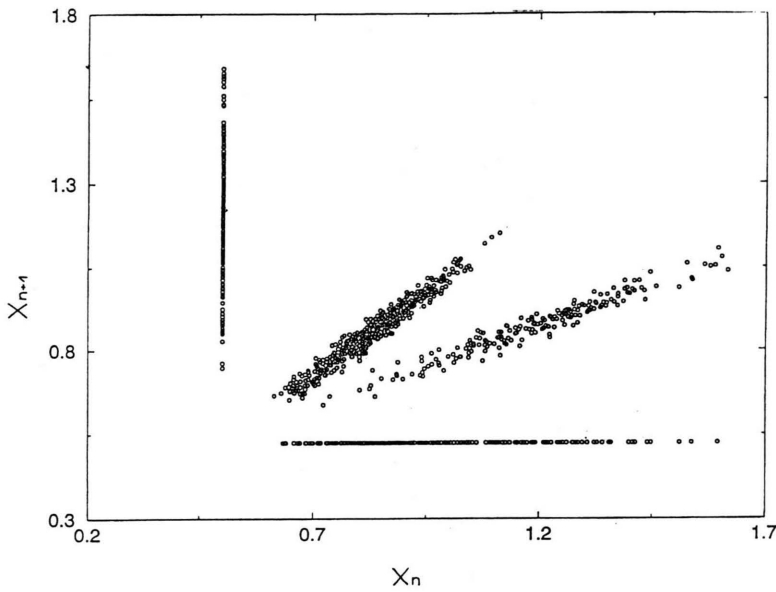


Fig. 3. Typical phase space diagram of class 1 and additional extrasystoles defined in class 2.

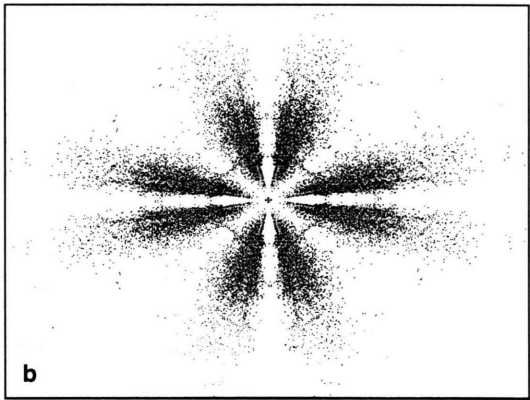
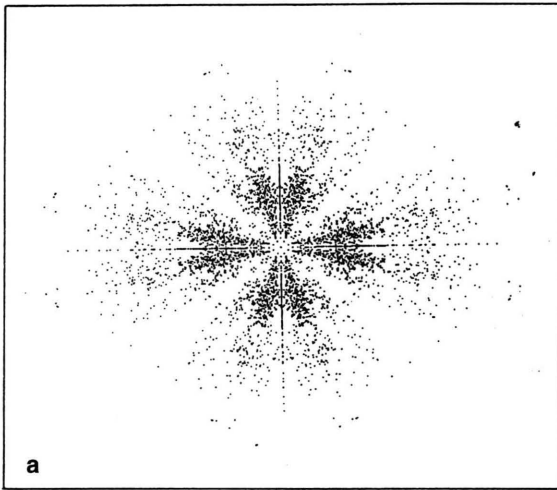


Fig. 4a. AIP diagram with artificial heart beat sequence as defined in class 2,  $c = 0.006$ ,  $\sigma = 0.02$ .

Fig. 4b. AIP diagram of real ECG data from a patient with ventricular extrasystoles.

systoles, where regular or irregular occurrence is reflected in the complexity of the structures in the phase space.

2. The AIP diagrams can serve as reliable diagnostic tools for recognizing different disturbances in the heart rhythm.

Now we are analysing the finer details of the AIP diagrams in order to more precisely distinguish the various disturbances in the heart rhythm. It is very promising to use color in generating the AIP diagrams.

The authors acknowledge the partial support of BW/5400-5-0303-7.

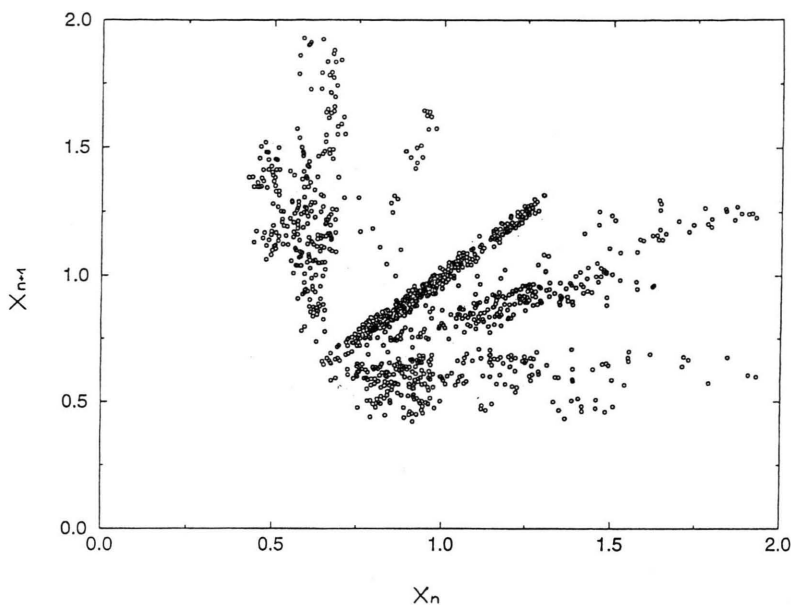


Fig. 5. A phase space diagram of model 1 with variable regular beat sequence and variable extrasystole as defined in class 3,  $c = 0.006$ ,  $\sigma = 0.02$ .

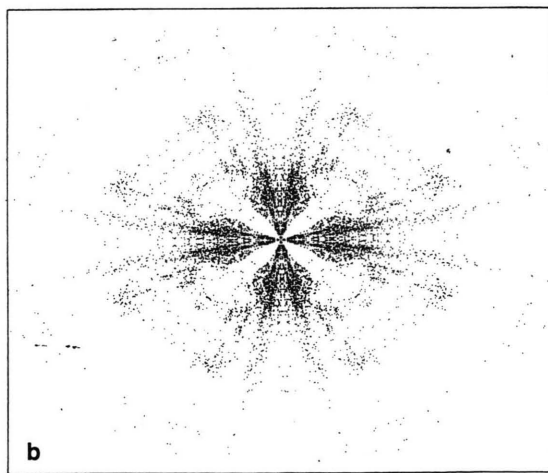
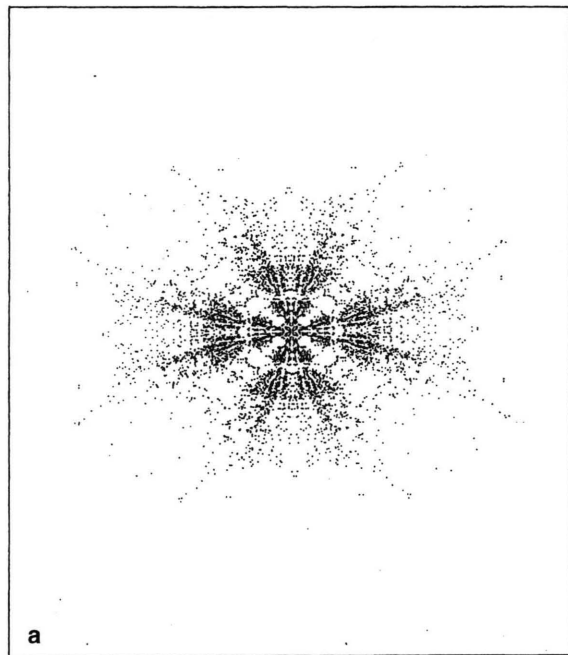


Fig. 6a. AIP diagram corresponding to the phase space diagram of previous figure.  
Fig. 6b. AIP diagram of real ECG data from severely ill patient.

- [1] P. Z. Saporin, M. A. Zaks, J. Kurths, A. Voss, and V. S. Anishchenko, *Phys. Rev. E* **54**, 737 (1996).
- [2] C. K. Peng, S. Havlin, H. E. Stanley, and A. L. Goldberger, *Chaos* **5**, 82 (1995).
- [3] J. J. Zebrowski, W. Popławska, and R. Baranowski, *Phys. Rev. E* **50**, 4187 (1994).
- [4] J. J. Zebrowski, W. Popławska, and R. Baranowski, *Acta Phys. Pol. B* **26**, 1055 (1995).
- [5] C. A. Pickover, *Computers, Pattern, Chaos, and Beauty*, (St. Martin's Press, New York 1990).
- [6] H. M. Jaenisch and C. A. Bjork, *Application of Synergetics to the Semi-Classical Tracking and Metric Discrimination Problem*. Nichols Research Corporation. POC: H. M. Jaenisch 1991.